Exchange and correlation potential for a two-dimensional electron gas at finite temperatures

S. Phatisena,* R. E. Amritkar, and P. V. Panat

Department of Physics, University of Poona, Ganeshkhind, Pune 411 007, Maharashtra, India

(Received 15 October 1985; revised manuscript received 18 June 1986)

Calculations for an inhomogeneous electron gas using density-functional theory require suitable exchange and correlation potentials. We present here the local exchange and correlation potential (V_{xc}) for the two-dimensional electron gas over a wide range of temperatures and densities based upon summation of ring graphs. A suitable parametric fit for V_{xc} is presented which is good to within 2% of the exact values. Various limits and graphs of the polarizability are presented.

I. INTRODUCTION

There has been a considerable surge of interest in the properties of two-dimensional (2D) electron gas (EG).[1] This is due to the fact that the electrons trapped on the liquid-helium surface or in the inversion or accumulation layer of metal-oxide-semiconductors (MOS) structures or in superlattice structures of GaAs-AlAs can be approximately modeled as a 2D EG. What is interesting is that the electron concentration of these two-dimensional layers can be varied to almost any level by appropriate doping in the semiconductors. Thus we get any situation from a nondegenerate to a highly degenerate electron gas in two dimensions[2] that has very large mobilities in the plane.

The density-functional theory has been very successful in the analysis of electronic properties of various inhomogeneous systems such as atoms, molecules, surfaces, etc. For a recent review of its various applications see Rajagopal.[3] The finite-temperature generalization of density-functional theory has been given by Mermin.[4] The finite-temperature theory is finding its use only recently. This is partly due to the fact that appropriate exchange and correlation potentials at intermediate degeneracy for three dimensions are appearing only recently.[5,6]

Study of the many-body properties of two-dimensional electron gas was initially done by Stern.[7,8] Subsequently, Isihara and his co-workers[9,10] and others[11] have extensively studied the many-body aspects of 2D EG at low temperatures. Thermodynamic potential (Ω) has been studied by Fetter[12] at high temperatures and he has obtained the equation of state and also the structure factor $S(q,\omega)$. Czachor et al.[13] have studied pair-correlation-function and plasmon-dispersion curves of 2D EG at $T=0$. Rajagopal et al.[14] have studied spin-polarized 2D EG in random-phase approximation (RPA) for possible paramagnetic and ferromagnetic ordering.

As was noted earlier, for 2D EG in a wide density range, we need the evaluation of exchange and correlation potential over a wide range of temperatures and densities. The impurity potential (IP) crucially depends on electron density, and IP is required for calculations of scattering cross section which in turn is required for the evaluation of mobility. It is also well known that the bound energy levels of impurity are affected by the presence of electron gas which in turn can be observed in x-ray photoelectron spectroscopy. The calculations of core-hole energies as well as the screening in the spirit of density-functional theory requires suitable, preferably local exchange and correlation potential. To our knowledge, so far, such potential is not available for 2D EG over a wide range of density and temperatures and hence this paper.

II. FORMALISM

Let us first consider the calculation of effective single-particle potential that enters in Kohn-Sham equations in exchange approximation. It is a functional derivative of thermodynamic potential (Ω_x) with respect to density (n). In Fock approximation, Ω_x is given as[15]

$$\Omega_x[n,T] = -\frac{2}{2A} \sum_{\mathbf{k},\mathbf{k}'} V(|\mathbf{k}-\mathbf{k}'|)\tilde{f}(k)\tilde{f}(k') , \qquad (1)$$

where $V(|\mathbf{k}-\mathbf{k}'|)$ is a Fourier transform of the Coulomb interaction in two dimensions. It is

$$V(|\mathbf{k}|) = 2\pi e^2/|\mathbf{k}| . \qquad (2)$$

The factor of 2 arises from spin degeneracy.

At absolute zero, $\tilde{f}(k)$, the Fermi functions, are Heaviside's Θ functions and at finite temperatures they are well-known Fermi factors

$$\tilde{f}(k) = [\exp(\varepsilon_k - \mu)\beta + 1]^{-1} , \qquad (3)$$

where $\varepsilon_k = \hbar^2 k^2/2m$ and μ is the chemical potential. Evolution of $\Omega_x[n,T]$ at zero temperature is elementary. It is

$$\Omega_x[n,T] = -\frac{2}{3}\frac{e^2 k_F^3}{\pi^2}, \quad T=0 \qquad (4a)$$

where

$$k_F = (2\pi n)^{1/2} .$$

In terms of r_s, the interparticle distance per Bohr radius, Ω_x is expressed as

$$\Omega_x[n, T=0] = -\frac{4\sqrt{2}}{3}\frac{e^2}{\pi^2} r_s^{-3} . \qquad (4b)$$

For finite temperatures, it is convenient to scale momenta, temperatures and chemical potential as $x = k/k_F$, $t = T/T_F$, and $\alpha = \mu/k_B T \equiv \beta\mu$, where T_F is the Fermi

temperature. Converting the sum over $\mathbf{k}$ and $\mathbf{k'}$ to an integral and carrying out the angular integrals, we transform Eq. (1) to

$$\frac{\Omega_x[n,t]}{\Omega_x[n,0]}=\frac{3}{2}\int\int\frac{xy}{x+y}K(\sqrt{4xy}/(x+y))$$

$$\times f(x)f(y)dx\,dy\ ,\qquad(5)$$

where

$$f(x)=(e^{x^2/t-\alpha}+1)^{-1}\qquad(6)$$

and $K(x)$ is the complete elliptic integral of the first kind which can be simplified as[16]

$$K(\sqrt{4xy}/(x+y))=\left[1+\frac{y}{x}\right]\Theta(x-y)K(y/x)$$

$$+\left[1+\frac{x}{y}\right]\Theta(y-x)K(x/y)\ .$$

Equation (5) then transforms to

$$\frac{\Omega_x[n,t]}{\Omega_x[n,0]}=3\int_0^\infty dx\,x^2f(x)\int_0^1dz\,zf(xz)K(z)\ .\qquad(7)$$

The exchange potential $V_x[n,t]$ is then given by

$$V_x[n,t]=\delta\Omega_x[n,t]/\delta n\ .\qquad(8)$$

Thus, from Eqs. (4), (7), and (8) we get

$$\frac{V_x[n,t]}{V_x[n,0]}=\frac{\Omega_x[n,t]}{\Omega_x[n,0]}-\frac{2}{t}\left[\int_0^\infty dx\,x^2f(x)\int_0^1dz\,f(xz)[1-f(xz)]z\left[x^2z^2-\frac{e^{1/t}}{e^{1/t}-1}\right]K(z)\right.$$

$$\left.+\int_0^\infty dx\,x^2f(x)[1-f(x)]\left[x^2-\frac{e^{1/t}}{e^{1/t}-1}\right]\int_0^1dz\,zf(xz)K(z)\right]\ .\qquad(9)$$

Here

$$V_x[n,0]=-\frac{2e^2}{\pi}(2\pi n)^{1/2}\ .\qquad(10)$$

The chemical potential $\mu=\alpha k_BT$, the reduced temperature t, and the density n are related by

$$n=\frac{2}{(2\pi)^2}\int d^2k\,\tilde{f}(k)\ .$$

The integral can be evaluated exactly to yield

$$\alpha=\ln(e^{1/t}-1)\ .\qquad(11)$$

At high and low temperatures α is very simply related to t by

$$\alpha\sim1/t\quad\text{as }t\to0\qquad(12a)$$

and

$$\alpha\sim-\ln t\quad\text{as }t\to\infty\ .\qquad(12b)$$

The low- and high-temperature limits of expressions (7) and (9) can be gotten with lengthy algebra (see Appendix A). Thus

$$\frac{\Omega_x[n,t]}{\Omega_x[n,0]}\to1+At^2+\frac{\pi^2}{16}t^2\ln t\quad\text{as }t\to0\qquad(13)$$

where

$$A=\frac{3}{2}\left[\frac{\pi^2}{12}\left[\frac{1}{2}-2\ln2\right]-\frac{\pi^2}{24}(1-\mathscr{C})+\frac{D}{2}+\frac{B}{4}\right]\ ,$$

$\mathscr{C}=0.577216\cdots$ is Enler's constant,

$$D=\sum_{k=1}^\infty\frac{(-1)^k}{k^2}\ln k\simeq-0.1013161\cdots\ ,$$

and

$$B=\int_0^\infty dx\frac{1}{e^x+1}\int_0^\infty dy\frac{1}{e^y+1}\ln\left|\frac{x+y}{x-y}\right|$$

$$\approx0.4224309\cdots\ .$$

The ratio $V_x[n,t]/V_x[n,0]$ behaves, in the same limit, as

$$\frac{V_x[n,t]}{V_x[n,0]}\to1-\frac{1}{3}\left[A+\frac{\pi^2}{8}\right]t^2-\frac{\pi^2}{48}t^2\ln t\quad\text{as }t\to0\ .$$

$$(14)$$

In the high-temperature limit

$$\frac{\Omega_x[n,t]}{\Omega_x[n,0]}\to\frac{2}{\sqrt{t}}A_2\quad\text{for }t\gg1\qquad(15)$$

where

$$A_2=\frac{\sqrt{\pi}}{8}\int_0^1\frac{K(z)}{(1+z)^{3/2}}dz\ .$$

The exchange potential is then

$$\frac{V_x[n,t]}{V_x[n,0]}\to4A_2t^{-1/2}\quad\text{for }t\gg1\ .\qquad(16)$$

The detailed plot for $\Omega_x[n,t]/\Omega_x[n,0]$ and $V_x[n,t]/V_x[n,0]$ is shown in Fig. 1. The low-temperature limit of Eq. (7) was also obtained by Isihara and Ioriatti.[10] However, our method of obtaining Eq. (13) is different from theirs and hence is presented in Appendix A.

Let us now calculate the correlation energy in random-phase approximation by summing the ring graphs. It is given by[15]

$$\Omega_c^{(r)} = \frac{L^2}{2\beta} \sum_{l=-\infty}^{\infty} \int_0^\infty dq \frac{q}{2\pi} \{\ln[1 - V(q)\Pi^{(0)}(q,\nu_l)]$$

$$+ V(q)\Pi^{(0)}(q,\nu_l)\} , \qquad (17)$$

where $\nu_l = 2\pi l/\beta\hbar$ and $l = 0,1,2,\ldots$.

$\Pi^{(0)}(q,\nu_l)$ is a proper part of the polarization propagator due to density fluctuation in the system. It has a form,

$$\Pi^{(0)}(\mathbf{q},\nu_l) = -2 \int \frac{d^2p}{(2\pi)^2} \frac{\tilde{f}(\mathbf{p+q}) - \tilde{f}(\mathbf{p})}{i\hbar\nu_l - (\varepsilon_{\mathbf{p+q}} - \varepsilon_{\mathbf{p}})} . \qquad (18)$$

This propagator can be analyzed for the static case ($\nu_l = 0$) and for the dynamic case ($\nu_l \neq 0$) separately. Equation (18) can be simplified for the static case to

$$\Pi^{(0)}(q,0) = \frac{2m}{\pi^2\hbar^2 q} \int_0^\infty dp\, p\tilde{f}(p) \int_0^{2\pi} d\theta \frac{1}{2p\cos\theta - q} .$$

The angular integral is easily carried out to lead to $-2\pi/(q^2 - 4p^2)^{1/2}$ with the upper limit of p integration
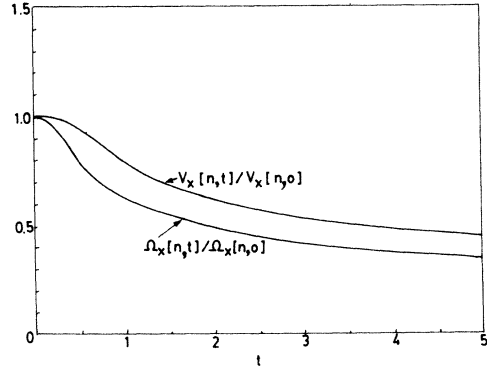

FIG. 1. Universal curves for scaled exchange part of thermodynamic potential $\Omega_x[n,t]/\Omega_x[n,0]$ and exchange potential $V_x[n,t]/V_x[n,0]$ vs t.

becoming $q/2$. Scaling q and p to $Q = q/k_F$ and $x = p/k_F$, respectively, the static part $\Pi^{(0)}(q,0)$ becomes

$$\Pi^{(0)}(Q,0) = -\frac{4m}{\pi\hbar^2 Q} \int_0^{Q/2} dx \frac{xf(x)}{(Q^2 - 4x^2)^{1/2}} . \qquad (19)$$

The dynamic polarization part on the other hand is

$$\Pi^{(0)}(q,\nu_l) = -\frac{m}{\pi^2\hbar^2 q} \int_0^\infty dp\, p\tilde{f}(p) \int_0^{2\pi} d\theta \left[\frac{1}{(q + 2p\cos\theta) + \dfrac{i\,2m\nu_l}{\hbar q}} + \text{c.c.} \right] ,$$

where c.c. denotes complex conjugate. The angular integral, by residue theorem, is $2\pi\cos\phi/pR$, where

$$R = \left\{ \left[\left[\frac{q}{2p} \right]^2 - \left[\frac{m\nu_l}{\hbar pq} \right]^2 - 1 \right]^2 + \left[\frac{m\nu_l}{\hbar p^2} \right]^2 \right\}^{1/4}$$

and

$$\tan(2\phi) = \frac{m\nu_l/\hbar p^2}{\left[\frac{q}{2p} \right]^2 - \left[\frac{m\nu_l}{\hbar pq} \right]^2 - 1} .$$

Upon scaling $Q = q/k_F$ and $x = p/k_F$, the dynamic polarization propagator becomes

$$\Pi^{(0)}(Q,\nu_l) = \frac{-4m}{\pi\hbar^2} \int_0^\infty dx \frac{xf(x)\cos\phi}{[(Q^4 - 4x^2Q^2 - 4l^2\pi^2t^2)^2 + 16l^2\pi^2t^2Q^4]^{1/4}} , \qquad (20)$$

where

$$\tan(2\phi) = \frac{4Q^2 l\pi t}{Q^4 - 4x^2Q^2 - 4l^2\pi^2t^2} . \qquad (21)$$

Following are the various limiting forms of $\Pi^{(0)}(Q,\nu_l)$ (in the units of $\hbar^2 = 2m = 1$, $e^2 = 2$).

   (a) Static polarization.

$$\Pi^{(0)}(Q) \to -\frac{1}{2\pi} + O(e^{-1/t}), \quad \text{as } t \to 0 \text{ for } Q \ll 2 \qquad (22a)$$

$$\Pi^{(0)}(Q) \to -\frac{1}{\pi Q^2} \left[1 + \frac{1}{Q^2} \left[1 + \frac{\pi^2 t^2}{3} \right] \right] ,$$

$$\text{as } t \to 0 \text{ for } Q \gg 2 \qquad (22b)$$

$$\Pi^{(0)}(Q) \to -\frac{1}{2\pi t} \left[1 - \frac{Q^2}{6t} \right], \quad \text{as } t \to \infty \text{ and } Q \to 0 \qquad (22c)$$
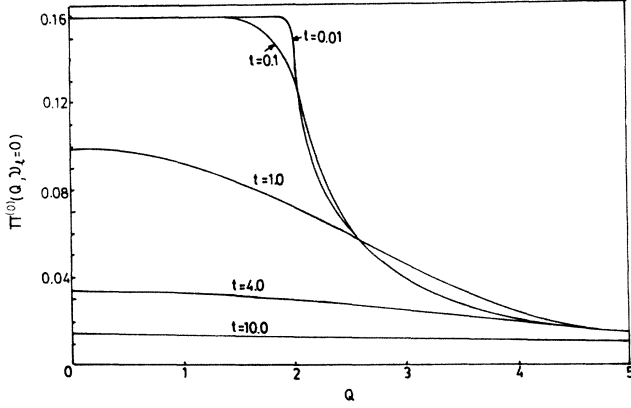
FIG. 2. Variation of static part of polarization propagator $\Pi^{(0)}(Q, \nu_l=0)$ with Q for various values of t.

$$\Pi^{(0)}(Q) \to -\frac{1}{\pi Q^2}\left[1+\frac{2t}{Q^2}\right],$$

$$\text{as } t\to\infty \text{ and } Q\to\infty \text{ for } t<Q^2 . \quad (22\text{d})$$

It must be noted that the polarization becomes independent of t as $Q\gg 1$. Figure 2 shows the behavior of $\Pi^{(0)}(Q, l=0)$ versus Q for different values of t.

(b) Dynamic polarization. In the case of dynamic polarization, a small Q limit can be obtained for all of the nonzero-t range. It is

$$\Pi^{(0)}(Q,\nu_l) \sim -\frac{1}{4\pi}\left[\frac{Q}{l\pi t}\right]^2 . \quad (23\text{a})$$

In the range of large Q values for any t,

$$\Pi^{(0)}(Q,\nu_l) = -\frac{2}{\pi Q^2}\left[\frac{1}{2}+\frac{t^2}{Q^2}\int_0^\infty dy\,\frac{y}{e^{y-\alpha}+1}\right] . \quad (23\text{b})$$

It is interesting to note that there is no l dependence in $\Pi^{(0)}(Q,\nu_l)$ for large Q. Equation (23b) can be easily analyzed for low- and high-t limits as

$$\Pi^{(0)}(Q,\nu_l) \to -\frac{1}{\pi Q^2}\left[1+\frac{1}{Q^2}\left[1+\frac{\pi^2 t^2}{3}\right]\right],$$

$$\text{as } t\to 0 \text{ for } Q\gg 1 \quad (23\text{c})$$

and

$$\Pi^{(0)}(Q,\nu_l) \to -\frac{1}{\pi Q^2}\left[1+\frac{2t}{Q^2}\right] \quad \text{for } 1\ll t<Q^2 . \quad (23\text{d})$$

Carrying angular integration and taking a functional derivative of Eq. (17) with respect to n, we obtain static and dynamic parts of the correlation potential as

$$V_c^{(r)}(l=0)=4k_F\left[\frac{e^{1/t}}{e^{1/t}-1}\right]\int_0^\infty dQ\,\frac{1}{Q}\left[\frac{V(Q)\Pi^{(0)}(Q)}{1-V(Q)\Pi^{(0)}(Q)}\right]\int_0^{Q/2}dx\,\frac{xf(x)[1-f(x)]}{(Q^2-4x^2)^{1/2}} \quad (24)$$

and

$$V_c^{(r)}(l\neq 0)=8k_F\left[\frac{e^{1/t}}{e^{1/t}-1}\right]$$

$$\times \sum_{l=1}^\infty \int_0^\infty dQ\,\frac{V(Q)\Pi^{(0)}(Q,\nu_l)}{1-V(Q)\Pi^{(0)}(Q,\nu_l)}g(Q,l,t) ,$$

$$(25)$$

where

$$V(Q)=4\pi/Qk_F$$

and

$$g(Q,l,t)$$

$$=\int_0^\infty dx\,\frac{xf(x)[1-f(x)]\cos\phi}{[(Q^4-4x^2Q^2-4l^2\pi^2 t^2)^2+16l^2\pi^2 t^2 Q^4]^{1/4}} .$$

The numerical values of $\Omega_c^{(r)}/N$, Ω_x/N, $V_c^{(r)}$, and V_x for the physically interesting range of r_s and t values are given in Table I. The total $\Omega_{xc}=\Omega_x+\Omega_c^{(r)}$ and $V_{xc}=V_x+V_c^{(r)}$ are also given in the table.

III. RESULTS AND DISCUSSION

Before we start discussing our results, it is to be noted that we have taken α to correspond to the noninteracting value of n. Corrections to α and to Ω are discussed by Dharma-Wardhana and Taylor.[5] However, it can be shown that these corrections are not important in the calculation of V_{xc}. Since our main interest here is the calculation of V_{xc}, we have not evaluated the correction factors.

It should be pointed out here that our results correspond to realistic semiconductor situations. The densities of electrons trapped on the surface of liquid He, which are of the order of 10^8 cm^{-2} are not the aim of the calculations of this paper. This is a very low density electron gas. Typical densities which exist in superlattices or at the interfaces of MOSFET junctions are of the order of 10^{11}–10^{14} cm^{-2}. The medium here is that of semiconductor, the effective mass m^* $(=\alpha m_e)$, and the Coulomb interactions are such that e^2 is scaled by e^2/ϵ_∞ and $m^*=\alpha m_e$ where ϵ_∞ is the static dielectric constant. Our calculations are made with a vacuum as medium. However, if we take the units

TABLE I. Values of the exchange-correlation potential V_{xc} and the thermodynamic potential Ω_{xc} as a function of t for several electron densities. Correlation and exchange contributions are also tabulated. (All units are Rydbergs.) (a), (b), (c), and (d) correspond to $r_s = 0.195$ ($n = 3 \times 10^{17}$ cm^{-2}); $r_s = 1.066$ ($n = 10^{16}$ cm^{-2}); $r_s = 3.372$ ($n = 10^{15}$ cm^{-2}); and $r_s = 4.998$ ($n = 4.55 \times 10^{14}$ cm^{-2}), respectively, when $\epsilon_\infty = 1$, $m^* = m$. Corresponding densities in realistic situation of semiconductor with $\epsilon_\infty = 8$, $m^* = 0.2m$ are $r_s = 0.195$ ($n = 1.87 \times 10^{14}$ cm^{-2}); $r_s = 1.066$ ($n = 6.26 \times 10^{12}$ cm^{-2}); $r_s = 3.372$ ($n = 6.25 \times 10^{11}$ cm^{-2}); and $r_s = 4.998$ ($n = 2.85 \times 10^{11}$ cm^{-2}).

t	$-\dfrac{\Omega_c^{(r)}}{N}$ $(l=0)$	$-\dfrac{\Omega_c^{(r)}}{N}$ $(l\neq0)$	$-\dfrac{\Omega_c^{(r)}}{N}$ (total)	$-\dfrac{\Omega_x}{N}$	$-\dfrac{\Omega_{xc}}{N}$	$-V_c^{(r)}$ $(l=0)$	$-V_c^{(r)}$ $(l\neq0)$	$-V_c^{(r)}$ (total)	$-V_x$	$-V_{xc}$
				(a) $r_s = 0.194\,654$ ($n = 3.0 \times 10^{17}$ cm^{-2})						
0.1	0.2660	0.3431	0.6091	6.0432	6.6523	0.0498	0.4845	0.5343	9.2504	9.7847
0.4	0.8812	0.1476	1.0288	5.1724	6.2012	0.5017	0.2706	0.7723	8.9082	9.6805
0.8	1.1612	0.0803	1.2415	4.2560	5.4975	1.1240	0.1550	1.2790	7.8101	9.0891
1.0	1.1956	0.0651	1.2607	3.9364	5.1971	1.2983	0.1265	1.4248	7.3365	8.7613
1.4	1.1885	0.0473	1.2358	3.4615	4.6973	1.4791	0.0927	1.5718	6.5734	8.1452
1.7	1.1557	0.0392	1.1949	3.1982	4.3931	1.5310	0.0772	1.6082	6.1266	7.7348
2.0	1.1150	0.0333	1.1483	2.9865	4.1348	1.5450	0.0658	1.6108	5.7556	7.3664
2.4	1.0581	0.0279	1.0860	2.7597	3.8457	1.5315	0.0552	1.5867	5.3504	6.9371
3.0	0.9768	0.0223	0.9991	2.4989	3.4980	1.4791	0.0443	1.5234	4.8741	6.3975
3.5	0.9159	0.0192	0.9351	2.3300	3.2651	1.4244	0.0381	1.4625	4.5597	6.0222
4.0	0.8616	0.0168	0.8784	2.1913	3.0697	1.3676	0.0334	1.4010	4.3005	5.7015
4.5	0.8131	0.0149	0.8280	2.0745	2.9025	1.3121	0.0297	1.3418	4.0789	5.4207
5.0	0.7699	0.0134	0.7833	1.9747	2.7580	1.2592	0.0267	1.2859	3.8898	5.1757
10.0	0.5083	0.0066	0.5149	1.2537	1.7686	0.8882	0.0133	0.9015	2.7994	3.7009
				(b) $r_s = 1.066\,16$ ($n = 1.0 \times 10^{16}$ cm^{-2})						
0.1	0.1264	0.2839	0.4103	1.1033	1.5136	0.0366	0.3972	0.4338	1.6889	2.1227
0.4	0.4227	0.1383	0.5610	0.9443	1.5053	0.2605	0.2477	0.5082	1.6264	2.1346
0.8	0.5887	0.0782	0.6669	0.7770	1.4439	0.5534	0.1490	0.7024	1.4259	2.1283
1.0	0.6226	0.0638	0.6864	0.7187	1.4051	0.6467	0.1227	0.7694	1.3395	2.1089
1.4	0.6478	0.0467	0.6945	0.6320	1.3265	0.7620	0.0909	0.8529	1.2001	2.0530
1.7	0.6479	0.0388	0.6867	0.5839	1.2706	0.8089	0.0761	0.8850	1.1185	2.0035
2.0	0.6402	0.0331	0.6733	0.5453	1.2186	0.8355	0.0651	0.9006	1.0508	1.9514
2.4	0.6240	0.0277	0.6517	0.5039	1.1556	0.8511	0.0547	0.9058	0.9768	1.8826
3.0	0.5949	0.0223	0.6172	0.4562	1.0734	0.8506	0.0441	0.8947	0.8899	1.7846
3.5	0.5699	0.0191	0.5890	0.4254	1.0144	0.8387	0.0379	0.8766	0.8325	1.7091
4.0	0.5459	0.0168	0.5627	0.4001	0.9628	0.8216	0.0333	0.8549	0.7852	1.6401
4.5	0.5233	0.0149	0.5382	0.3788	0.9170	0.8020	0.0296	0.8316	0.7447	1.5763
5.0	0.5022	0.0134	0.5156	0.3605	0.8761	0.7814	0.0267	0.8081	0.7102	1.5183
10.0	0.3587	0.0067	0.3654	0.2289	0.5943	0.6023	0.0133	0.6156	0.5111	1.1267
				(c) $r_s = 3.3715$ ($n = 1.0 \times 10^{15}$ cm^{-2})						
0.1	0.0619	0.2124	0.2743	0.3489	0.6232	0.0226	0.2956	0.3182	0.5341	0.8523
0.4	0.2114	0.1208	0.3322	0.2986	0.6308	0.1353	0.2079	0.3432	0.5143	0.8575
0.8	0.3099	0.0732	0.3831	0.2457	0.6288	0.2818	0.1360	0.4178	0.4509	0.8687
1.0	0.3357	0.0607	0.3964	0.2273	0.6237	0.3333	0.1144	0.4477	0.4236	0.8713
1.4	0.3639	0.0452	0.4091	0.1998	0.6089	0.4046	0.0868	0.4914	0.3795	0.8709
1.7	0.3735	0.0379	0.4114	0.1847	0.5961	0.4393	0.0734	0.5127	0.3537	0.8664
2.0	0.3774	0.0325	0.4099	0.1724	0.5823	0.4634	0.0632	0.5266	0.3323	0.8589
2.4	0.3774	0.0273	0.4047	0.1593	0.5640	0.4842	0.0535	0.5377	0.3089	0.8466
3.0	0.3713	0.0220	0.3933	0.1443	0.5376	0.4999	0.0433	0.5432	0.2814	0.8246
3.5	0.3635	0.0190	0.3825	0.1345	0.5170	0.5044	0.0374	0.5418	0.2633	0.8051
4.0	0.3546	0.0166	0.3712	0.1265	0.4977	0.5041	0.0329	0.5370	0.2482	0.7852
4.5	0.3453	0.0148	0.3601	0.1198	0.4799	0.5009	0.0293	0.5302	0.2355	0.7657
5.0	0.3360	0.0133	0.3493	0.1140	0.4633	0.4956	0.0264	0.5220	0.2246	0.7466
10.0	0.2603	0.0066	0.2669	0.0724	0.3393	0.4196	0.0132	0.4328	0.1616	0.5944
				(d) $r_s = 4.998\,255$ ($n = 4.55 \times 10^{14}$ cm^{-2})						
0.1	0.0467	0.1865	0.2332	0.2353	0.4685	0.0180	0.2564	0.2744	0.3603	0.6347
0.4	0.1608	0.1124	0.2732	0.2014	0.4746	0.1037	0.1889	0.2926	0.3469	0.6395
0.8	0.2400	0.0709	0.3109	0.1657	0.4766	0.2154	0.1286	0.3440	0.3042	0.6482
1.0	0.2621	0.0588	0.3209	0.1532	0.4741	0.2558	0.1094	0.3652	0.2857	0.6509
1.4	0.2884	0.0443	0.3327	0.1348	0.4675	0.3138	0.0843	0.3981	0.2560	0.6541

TABLE I. (*Continued*).

t	$-\dfrac{\Omega_c^{(r)}}{N}$ ($l=0$)	$-\dfrac{\Omega_c^{(r)}}{N}$ ($l\neq0$)	$-\dfrac{\Omega_c^{(r)}}{N}$ (total)	$-\dfrac{\Omega_x}{N}$	$-\dfrac{\Omega_{xc}}{N}$	$-V_c^{(r)}$ ($l=0$)	$-V_c^{(r)}$ ($l\neq0$)	$-V_c^{(r)}$ (total)	$-V_x$	$-V_{xc}$
1.7	0.2988	0.0372	0.3360	0.1245	0.4605	0.3434	0.0716	0.4150	0.2386	0.6536
2.0	0.3044	0.0321	0.3365	0.1163	0.4528	0.3649	0.0622	0.4271	0.2241	0.6512
2.4	0.3074	0.0270	0.3344	0.1075	0.4419	0.3847	0.0527	0.4374	0.2084	0.6458
3.0	0.3061	0.0219	0.3280	0.0973	0.4253	0.4021	0.0429	0.4450	0.1898	0.6348
3.5	0.3022	0.0188	0.3210	0.0907	0.4117	0.4093	0.0370	0.4463	0.1776	0.6239
4.0	0.2970	0.0165	0.3135	0.0853	0.3988	0.4122	0.0326	0.4448	0.1675	0.6123
4.5	0.2911	0.0147	0.3058	0.0808	0.3866	0.4124	0.0291	0.4415	0.1588	0.6003
5.0	0.2848	0.0133	0.2981	0.0769	0.3750	0.4106	0.0263	0.4369	0.1515	0.5884
10.0	0.2283	0.0066	0.2349	0.0488	0.2837	0.3615	0.0131	0.3746	0.1090	0.4836

$$\frac{e^2}{\epsilon_\infty}=2, \quad \hbar^2=1=2m^*=2\alpha m_e \; ,$$

then the Bohr radius is (ϵ_∞/α) times 0.529×10^{-8} cm and the unit of energy is $(\alpha/\epsilon_\infty^2)\times13.6$ eV. Under these circumstances $a_0^*=(\epsilon_\infty/\alpha)a_0$ and the redefined $r_s=(1.0665\times10^8/\sqrt{n})\,\alpha/\epsilon_\infty$ where n is the number of carriers per square centimeter. Typical, in the semiconductor inversion layer[17] $\epsilon_\infty\sim8$, $\alpha\sim0.2$. For this particular case, we easily see that when the above values of dielectric constant and effective mass are used the r_s and T_F values for various realistic densities can be calculated. Typical values of r_s and T_F are given in Table II. Our fitted formula for V_{xc} can be directly used with appropriate r_s and T_F values and the corresponding energy unit.

The experiments on heterojunctions are usually done below 100 K. The values of T_F critically depend upon the medium through m^* and ϵ_∞. As can be seen from Table II, at such temperatures any degree of degeneracy is possible. The region of intermediate degeneracy $(1 \lesssim t \lesssim 10)$ is inaccessible by any limiting formula. The value of our work lies in giving V_{xc} in parametric form for the range of intermediate degeneracy.

Let us start by considering the exchange contribution to the potential as shown in Fig. 1. The curves in Fig. 1 are the universal functions of the variable t and are independent of n. This is the artifact of the exchange model and the similar result is also obtained in three dimensions.[18] In the quantum regime, i.e., $t\ll1$, $V_x[n,t]$ is approximately constant and tends to zero slowly as $t^{-1/2}$ when $t\gg1$ [see Eqs. (14) and (16)]. The limiting behavior for small t agrees with that given by Isihara and Toyoda.[9] The effect of exchange is normally not included for $t\gg1$. However, our result shows that the exchange contribution is not negligible.

The behavior of the static and dynamic parts of polarization as a function of Q are shown in Figs. 2 and 3, respectively. The various limits of $\Pi^{(0)}$ have been already given in Eqs. (22) and (23). Static part of $\Pi^{(0)}$ is approximately constant up to $Q=2$, its value being 0.159 in the low temperature limit. This behavior is in agreement with that calculated by Maldague.[17] Contrary to the static part, the dynamical polarization goes to zero for all t at

$Q=0$. It is seen from Fig. 3 that the peak in $\Pi^{(0)}(Q,\nu_l)$ shifts to larger values of Q as l increases and also as t increases. The widths of the peaks in $\Pi^{(0)}(Q,\nu_l)$ become broader with increasing l and increasing t.

Numerical evaluation of Eqs. (24) and (25) has been carried out for various values of n and t and the total correlation potential is displayed in Fig. 4 for three typical densities as a function of t. The exchange potential is also displayed for comparison in the same figure. It is seen from the figure that the exchange part dominates over correlation at smaller values of t and the behavior is reversed for large t values. The crossover of the dominance of exchange over correlation occurs approximately near the degeneracy temperature. The crossover temperature t_0 shifts to higher values as the density increases. A similar behavior is noted in the three-dimensional case by Gupta and Rajagopal.[6] Our results of $\Omega_c^{(r)}$ at low temperatures agree with those of Isihara and Toyoda[9] and they agree with those of Fetter[12] in the high-t limit.

In general, evaluation of Eqs. (24) and (25) is fairly complicated, particularly at low t because of the sharp fall of $f(x)$. This difficulty has been overcome by dividing the range of integration into different parts depending on the shape of $f(x)$ and $\Pi^{(0)}(Q,\nu_l)$. The 32-point Gaussian quadrature was used to carry out the integrations. Evaluation of $V_c^{(r)}$ is further complicated by the infinite

TABLE II. Values of realistic densities that occur in semiconductor 2D EG. Densities are in cm^{-2} and corresponding values of r_s and T_F are calculated with $\epsilon_\infty=8$, $m^*=0.2m$. The conversion factors are $r_s=(1.0665\times10^8/\sqrt{n})(\alpha/\epsilon_\infty)$, unit of energy is $R_{yd}^*=13.6(\alpha/\epsilon_\infty^2)$ eV, $T_F=(0.316066\times10^6/r_s^2)(\alpha/\epsilon_\infty^2)$.

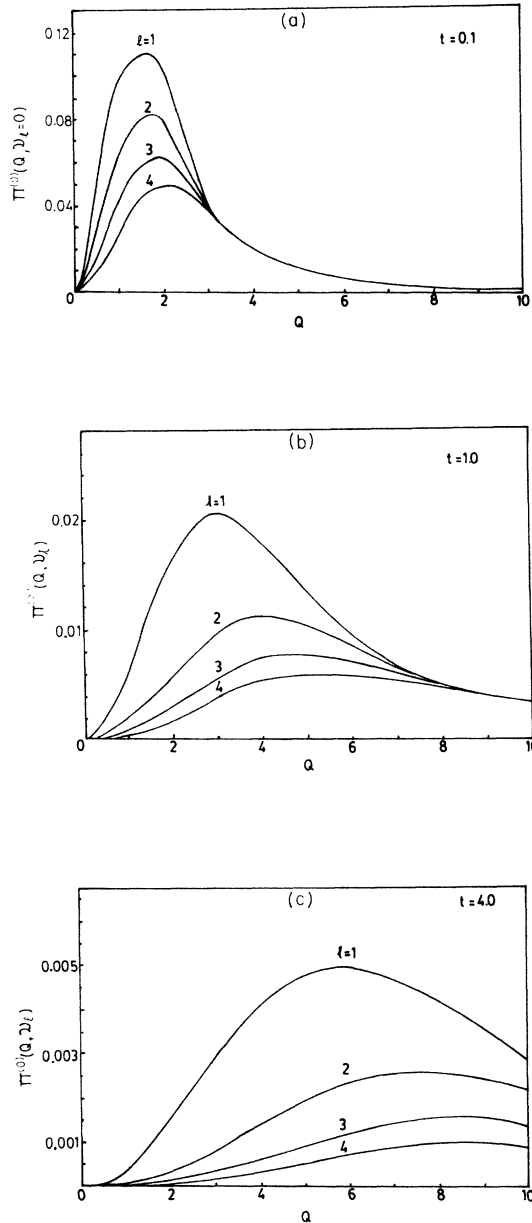| Density (cm^{-2})	r_s	T_F
10^{11}	8.43	13.89
2×10^{11}	5.96	27.79
5×10^{11}	3.77	69.47
10^{12}	2.67	138.94
10^{13}	0.84	1389.40
5×10^{13}	0.38	6947.70
10^{14}	0.27	13 894.00

FIG. 3. Dynamical part of polarization propagator $\Pi^{(0)}(Q,\nu_l)$ as a function of Q. Curves are labeled by l. (a) corresponds to $t=0.1$, (b) to $t=1.0$, and (c) to $t=4$.

sum over the l values. At low temperatures, the convergence of the series is low and therefore a large number of l values were required, e.g., at $t=0.1$, $l_{max}=200$ was used. Also, corrections from $l > l_{max}$ were estimated and added to the result by treating l as a continuous variable. For large t values convergence is fairly good. For $t=5$, $l_{max}=20$ is adequate. It is to be noted from Table I that the contribution from the static part ($l=0$ term) dominates at high temperature while the contribution from the dynamic part dominates at low temperature.

Figure 5 shows our final result of V_{xc} $[n,t]/V_x[n,0]$ versus t for ten different values of r_s. It should be noted
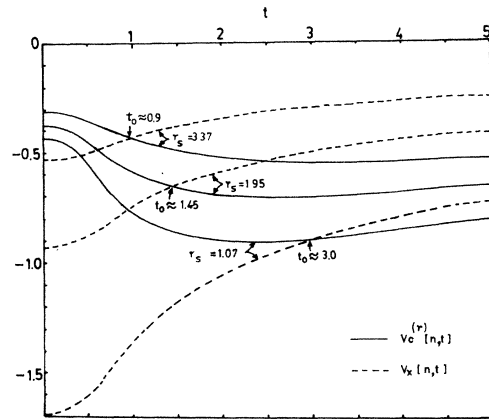

FIG. 4. $V_c^{(r)}[n,t]$ (solid curves) and $V_x[n,t]$ (dashed curves) as a function of t for three different r_s.

in Fig. 5 that there is a mild peak near about $t \sim 1$ which shifts to lower values of t with decreasing r_s. A similar behavior has been obtained by Perrot and Dharma-wardana[21] (see their Fig. 1) for the case of three dimensions.

As can be seen from Figs. 4 and 5, the $t^2\ln t$ term in exchange [see Eq. (14)] at low temperatures is almost canceled by the correlation part, at least numerically. A similar cancellation is also obtained in the three-dimensional case.[19-21] This is an important verification of the accuracy of the numerical work.

The values of $V_{xc}[n,t]/V_x[n,0]$ as a function of n and t were fitted by Lorentzian shape. The agreement between the fitted values and the calculated values, as can be seen from Table III, is excellent. The maximum error is about 4% for small r_s and the fit is better than 2% for $r_s > 0.2$. The overall average error is less than 1% where the chi square (χ^2) is 0.0059 for 130 values. The numerical values of constants of the fit are given in Appendix B.

Finally, some comments regarding the validity of RPA in two dimensions are in order. In RPA each electron
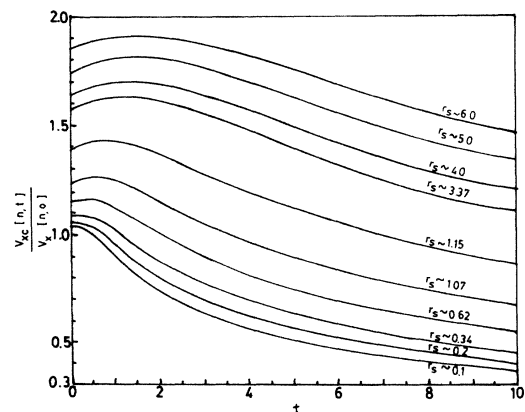

FIG. 5. $V_{xc}[n,t]/V_x[n,0]$ as a function of t for ten different r_s values.

TABLE III. Comparison of calculated values of $V_{xc}[n,t]/V_x[n,0]$ with those obtained by fitting formulas (B1) for several physically interesting densities.

t	$r_s=0.19$ Calculated	Fitted	$r_s=1.06$ Calculated	Fitted	$r_s=3.37$ Calculated	Fitted	$r_s=5.0$ Calculated	Fitted
0.1	1.0578	1.0632	1.2569	1.2499	1.5957	1.5912	1.7619	1.7631
0.4	1.0465	1.0458	1.2639	1.2539	1.6056	1.6089	1.7754	1.7799
0.8	0.9826	0.9964	1.2602	1.2470	1.6266	1.6255	1.7992	1.7982
1.0	0.9471	0.9647	1.2487	1.2385	1.6312	1.6301	1.8068	1.8049
1.4	0.8805	0.8962	1.2156	1.2131	1.6308	1.6316	1.8156	1.8127
1.7	0.8362	0.8460	1.1863	1.1881	1.6223	1.6257	1.8141	1.8130
2.0	0.7963	0.7998	1.1554	1.1597	1.6082	1.6142	1.8077	1.8086
2.4	0.7499	0.7462	1.1148	1.1191	1.5852	1.5917	1.7927	1.7959
3.0	0.6916	0.6831	1.0566	1.0575	1.5441	1.5473	1.7623	1.7655
3.5	0.6510	0.6437	1.0119	1.0097	1.5075	1.5061	1.7316	1.7342
4.0	0.6164	0.6134	0.9711	0.9667	1.4704	1.4651	1.6997	1.7012
4.5	0.5860	0.5900	0.9334	0.9292	1.4336	1.4267	1.6665	1.6693
5.0	0.5595	0.5718	0.8989	0.8969	1.3981	1.3921	1.6334	1.6398

moves in the Hartree field of all other electrons. The RPA is very successful in the long-wavelength limit in explaining plasmon modes and screening. However, RPA has some shortcomings. It does not take short-range correlations into account adequately. Jonson[22] has shown that RPA is less satisfactory in two dimensions than in three dimensions. The analysis presented by Jonson is valid for $T=0$. Since RPA fails to describe short-range correlations, the pair-correlation function $g(r)$ does not go to the value $\frac{1}{2}$ but becomes negative at $r=0$. As a matter of fact this negativeness of $g(r)$ around $r=0$ is more pronounced in two dimensions than in three dimensions. Various different remedies have been suggested to improve RPA results. To take exchange contribution to the dielectric constant into account, one writes

$$\epsilon(q,\omega)=1-V(q)\Pi(q,\omega)[1-G(q)] ,$$

where $G(q)$ is a correction factor; clearly with $G(q)=0$ we recover the RPA result.

Different forms of $G(q)$ give different approximations. Historically Hubbard was the first to give a correction to RPA in three dimensions. However, one of the best corrections to RPA is due to Singwi, Tosi, Land, and Söllander[23] (STLS), whereby $g(r)$ turns out to be positive around $r\approx0$ in three dimensions. Similar results are true in two dimensions also. Jonson compares RPA, Hubbard, and STLS approximations to the correlation part of internal energy in two dimensions. We have plotted E_c as a function of r_s of the result. Clearly V_c is proportional to dE_c/dr_s. The $T=0$ results indicate that, if we assume STLS results are correct, then V_c is overestimated by about 30–40 % by RPA in the range of r_s under considerations in two dimensions. There is no detailed investigation of this problem at finite temperature. We have not done such detailed investigation at finite temperatures but we believe that similar trends may persist.

Then there is one more problem of charge-density wave (CDW). Maldague[24] has investigated first-order exchange to polarization propagator at $T=0$. He finds that $\Pi^{(1)}(q)$ has a sharp cusplike peak at $q=2k_F$. At this point

$\Pi^{(0)}(q)$ falls monotonically. In three dimensions, however, $\Pi^{(1)}(q)$ has no sharp cusplike singularity. From Maldague's analysis, it appears that in two dimensions $\Pi^{(1)}(2k_F)$ exceeds $\Pi^{(0)}(2k_F)$ for $r_s\geq1$. There are "ladder" contributions[25] to $\Pi(q)$ and they are approximately taken into account by Maldague.[24] The analysis shows that $\Pi(q)$ is singular for $r_s\simeq0.9$. This certainly will be reflected in Ω and V. There is no detailed analysis, however. At finite temperatures we expect that such singularities will be blunted out and we feel that RPA will not be as bad. At least so far, no CDW is positively observed experimentally. In our paper, we have initially used finite temperature RPA for 2D EG and our $V_{xc}[n,T]$ should at least be useful as an initial starting potential for local-density-functional calculations.

As indicated in the Introduction, the present calculation will be useful to obtain the nonlinear response of electrons due to impurity as well as the binding energies. The calculations in these directions are in progress.

APPENDIX A: LOW- AND HIGH-TEMPERATURE LIMITS OF $\Omega_x[n,t]$ AND $V_x[n,t]$

Low temperatures. Equation (5) for $\Omega_x[n,t]$ can be written as

$$\frac{\Omega_x[n,t]}{\Omega_x[n,0]}=\frac{3}{8}t^{3/2}\int_0^\infty du\frac{1}{e^{u-\alpha}+1}\int_0^\infty dv\frac{1}{e^{v-\alpha}+1}g(u,v)$$

$$=\frac{3}{8}t^{3/2}I(t) , \tag{A1}$$

where we have used $x^2/t=u$ and $y^2/t=v$ and

$$g(u,v) = \frac{K(2(uv)^{1/4}/(\sqrt{u}+\sqrt{v}))}{\sqrt{u}+\sqrt{v}} .$$

The Fermi functions in (A1) can be simplified as

$$\int_0^\infty dx \frac{1}{e^{x-\alpha}+1} = \int_0^\alpha dx - \int_0^\alpha dx \frac{1}{e^{\alpha-x}+1} + \int_\alpha^\infty dx \frac{1}{e^{x-\alpha}+1}$$

and thus we get

$$I(t) = I_1(t) + I_2(t) + I_3(t) + I_4(t) \cdots , \tag{A2}$$

where

$$I_1(t) = \int_0^\alpha du \int_0^\alpha dv\, g(u,v) ,$$

$$I_2(t) = -2 \int_0^\alpha du \int_0^\alpha dv \frac{1}{e^{\alpha-v}+1} g(u,v) ,$$

$$I_3(t) = 2 \int_0^\alpha du \int_\alpha^\infty dv \frac{1}{e^{v-\alpha}+1} g(u,v) ,$$

$$I_4(t) = \left[\int_0^\alpha du \frac{1}{e^{\alpha-u}+1} - \int_\alpha^\infty du \frac{1}{e^{u-\alpha}+1} \right]$$

$$\times \left[\int_0^\alpha dv \frac{1}{e^{\alpha-v}+1} - \int_\alpha^\infty dv \frac{1}{e^{v-\alpha}+1} \right] g(u,v) .$$

The term I_1 simply becomes $8\alpha^{3/2}/3$. The second and the third terms I_2 and I_3 can be simplified by using the substitutions $\alpha-v=z$ and $v-\alpha=z$, respectively. Carrying out the u integral we get

$$I_2 = -4\sqrt{\alpha} \int_0^\alpha dz \frac{1}{e^z+1} E\sqrt{\alpha-z}/\sqrt{\alpha} ,$$

$$I_3 = 4 \int_0^\infty dz \frac{1}{e^z+1} \left[\sqrt{\alpha+z} E(\sqrt{\alpha/(\alpha+z)}) \right.$$

$$\left. - \frac{z}{\sqrt{\alpha+z}} K(\sqrt{\alpha/(\alpha+z)}) \right] ,$$

where E is the elliptic integral of the second kind. The upper limit in the integration I_2 can be approximated to ∞ with only exponential errors. The elliptic integrals have the series expansions[16]

$$E(z) = 1 + \frac{1}{2} \left[\ln \left[\frac{4}{z'} \right] - \frac{1}{1\times 2} \right] z'^2$$

$$+ \frac{1^2 \times 3}{2^2 \times 4} \left[\ln \left[\frac{4}{z'} \right] - \frac{2}{1\times 2} - \frac{1}{3\times 4} \right] z'^4 + \cdots ,$$

$$K(z) = \ln \left[\frac{4}{z'} \right] + \left[\frac{1}{2} \right]^2 \left[\ln \left[\frac{4}{z'} \right] - \frac{2}{1\times 2} \right] z'^2$$

$$+ \left[\frac{1\times 3}{2\times 4} \right]^2 \left[\ln \left[\frac{4}{z'} \right] - \frac{2}{1\times 2} - \frac{2}{3\times 4} \right] z'^4 + \cdots ,$$

where

$$z' = (1-z^2)^{1/2} .$$

Retaining only the lowest-order terms, we get

$$I_2 + I_3 \approx 4 \int_0^\infty dz \frac{1}{e^z+1} \frac{z}{\sqrt{\alpha}} \left[\frac{1}{2} - 2\ln 2 - \frac{1}{2}\ln z + \frac{1}{2}\ln\alpha \right]$$

$$= \frac{4}{\sqrt{\alpha}} \left[\frac{\pi^2}{12} \left[\frac{1}{2} - 2\ln 2 \right] - \frac{\pi^2}{24}(1-\mathscr{C}) + \frac{D}{2} \right]$$

$$- \frac{\pi^2}{6} \frac{\ln\alpha}{\sqrt{\alpha}} ,$$

where the constant $\mathscr{C}$ and D are given in Sec. II.

To calculate I_4 we use the same procedure as in I_2 and I_3 and after some algebra

$$I_4 \approx \frac{1}{\sqrt{\alpha}} \int_0^\infty d\xi \frac{1}{e^\xi+1} \int_0^\infty d\eta \frac{1}{e^\eta+1} \ln \left| \frac{\xi+\eta}{\xi-\eta} \right|$$

$$= \frac{B}{\sqrt{\alpha}} ,$$

where B is given by Eq. (13).

Adding I_1, I_2, I_3, and I_4 and with $\alpha \sim 1/t$ we get Eq. (13) and the corresponding Eq. (14). The high-temperature limit is obtained by using a straightforward procedure and hence not discussed.

APPENDIX B: CURVE FITTING OF $V_{xc}[n,t]/V_x[n,0]$

The ratio $V_{xc}[n,t]/V_x[n,0]$ at various r_s and t is tabulated in Table III. The simple Lorentzian equation to fit this ratio is of the form

$$\frac{V_{xc}[n,t]}{V_x[n,0]} = A(r_s) + \frac{B(r_s)}{[t-t_0(r_s)]^2 + C^2(r_s)} , \tag{B1}$$

where

$$A(r_s) = a_A + b_A r_s - c_A r_s^2 ,$$

$$B(r_s) = a_B - b_B r_s + c_B \tanh(d_B r_s) ,$$

$$C(r_s) = a_C + b_C \tanh(c_C r_s) ,$$

$$t_0(r_s) = a_T + b_T r_s - c_T r_s^2 ,$$

and t_0 is the maximum of the ratio. The numerical fitting values are as follows:

$$a_A = 0.428\,837, \quad b_A = 0.238\,679 ,$$

$$c_A = 0.007\,816, \quad a_B = 1.142\,037 ,$$

$$b_B = 0.899\,895, \quad c_B = 8.949\,627 ,$$

$$d_B = 1.123\,990, \quad a_C = 1.582\,764 ,$$

$$b_C = 2.219\,435, \quad c_C = 1.507\,691 ,$$

$$a_T = -0.153\,783, \quad b_T = 0.567\,801 ,$$

and

$$c_T = 0.044\,602 .$$

The values obtained using Eq. (B1) are tabulated in Table III.

*Present address: Department of Physics, Ubol Teacher College, Ubol Ratchathani 3, Thailand.

[1]T. Ando, A. B. Fowler, and F. Stern, Rev. Mod. Phys. 54, 437 (1982).

[2]H. L. Stormer, J. Phys. Soc. Jpn. Suppl. 49, A1013 (1980).

[3]A. K. Rajagopal, Adv. Chem. Phys. 41, 59 (1980).

[4]N. D. Mermin, Phys. Rev. 137, A1441 (1965).

[5]M. W. C. Dharma-wardana and R. Taylor, J. Phys. C 14, 629 (1981).

[6]U. Gupta and A. K. Rajagopal, Phys. Rev. A 22, 2792 (1980).

[7]F. Stern, Phys. Rev. Lett. 18, 546 (1967).

[8]F. Stern and W. E. Howard, Phys. Rev. 163, 816 (1967).

[9]A. Isihara and T. Toyoda, Phys. Rev. B 21, 3358 (1980).

[10]A. Isihara and L. Ioriatti, Physica A 103, 621 (1980).

[11]A. K. Rajagopal and J. C. Kimball, Phys. Rev. B 15, 2819 (1977).

[12]A. L. Fetter, Phys. Rev. B 10, 3739 (1974).

[13]A. Czachor, A. Holas, S. R. Sharma, and K. S. Singwi, Phys. Rev. B 25, 2145 (1982). See also K. S. Singwi and M. P. Tosi, in Solid State Physics 36, 177 (1981).

[14]A. K. Rajagopal, S. P. Singhal, M. Banerjee, and J. C. Kimball, Phys. Rev. B 17, 2262 (1978).

[15]A. L. Fetter and J. D. Walecka, Quantum Theory of Many-Particle Systems (McGraw-Hill, New York, 1971), p. 269.

[16]I. S. Gradshteyn and I. M. Ryzhik, Table of Integrals, Series and Product (Academic, London, 1965).

[17]P. F. Maldague, Surf. Sci. 73, 296 (1978).

[18]Uday Gupta and A. K. Rajagopal, Phys. Rev. A 21, 2064 (1980).

[19]D. G. Kanhere, P. V. Panat, A. K. Rajagopal, and J. Callaway, Phys. Rev. A 33, 490 (1986).

[20]W. Kohn and P. Vashishta, in Theory of the Inhomogeneous Electron Gas, edited by S. Lundqvist and N. H. March (Plenum, New York, 1983), p. 79.

[21]F. Perrot and M. W. C. Dharma-wardana, Phys. Rev. A 30, 2619 (1984).

[22]M. Jonson, J. Phys. C 9, 3055 (1976).

[23]K. S. Singwi, L. P. Tosi, R. H. Land, and A. Söllander, Phys. Rev. 176, 589 (1968).

[24]P. F. Maldague, Solid State Commun. 26, 133 (1978); see also P. F. Maldague and D. M. Nicholson, Physica (Utrecht) 99B, 250 (1980).

[25]A. K. Rajagopal, Phys. Rev. A 6, 1239 (1972).

[26]A. Isihara and T. Toyoda, Z. Phys. B 23, 389 (1976).

[27]A. H. Sommerfeld and H. Bethe, Vol. 24 of Handbuch der Physik (Springer-Verlag, Berlin, 1933), p. 346.